

# Bipedal Robotic Running with DURUS-2D: Bridging the Gap between Theory and Experiment \*

Wen-Loong Ma  
California Institute of  
Technology  
Pasadena, CA  
wma@caltech.edu

Shishir Kolathaya  
California Institute of  
Technology  
Pasadena, CA  
sny@caltech.edu

Eric R. Ambrose  
California Institute of  
Technology  
Pasadena, CA  
eamrose@caltech.edu

Christian M. Hubicki  
Georgia Institute of  
Technology  
Atlanta, GA  
chubicki6@gatech.edu

Aaron D. Ames  
California Institute of  
Technology  
Pasadena, CA  
ames@cds.caltech.edu

## ABSTRACT

Bipedal robotic running remains a challenging benchmark in the field of control and robotics because of its highly dynamic nature and necessarily underactuated hybrid dynamics. Previous results have achieved bipedal running experimentally with a combination of theoretical results and heuristic application thereof. In particular, formal analysis of the hybrid system stability is given based on a theoretical model, but due to the gap between theoretical concepts and experimental reality, extensive tuning is necessary to achieve experimental success. In this paper, we present a formal approach to bridge this gap, starting from theoretical gait generation to a provably stable control implementation, resulting in bipedal robotic running. We first use a large-scale optimization to generate an energy-efficient running gait, subject to hybrid zero dynamics conditions and feasibility constraints which incorporate practical limitations of the robot model based on physical conditions. The stability of the gait is formally guaranteed in the hybrid system model with an input to state stability (ISS) based control law. This implementation improves the stability under practical control limitations of the system. Finally, the methodology is experimentally realized on the planar spring-legged bipedal robot, DURUS-2D, resulting in sustainable running at 1.75 m/s. The paper, therefore, presents a formal method that takes the first step toward bridging the gap between theory and experiment.

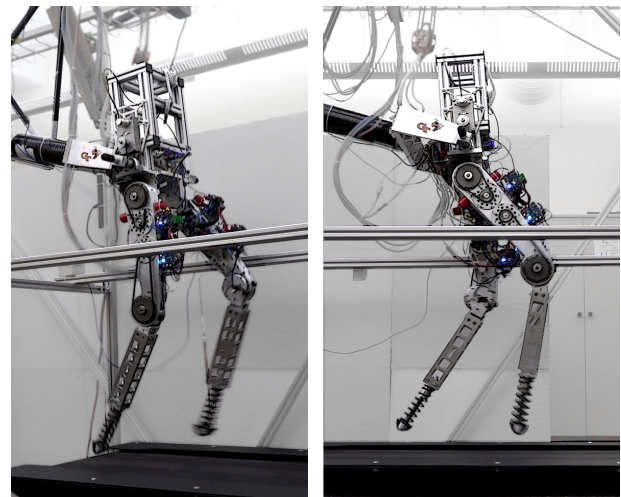


Figure 1: The spring-legged planar running biped, DURUS-2D, during take off (left) and while airborne (right).

## CCS Concepts

•Theory of computation → Numeric approximation algorithms; Convex optimization; •Computer systems organization → Robotic control; •Applied computing → Physical sciences and engineering;

## Keywords

Bipedal running; multi-domain hybrid systems; hybrid zero dynamics; nonlinear programming; input to state stability.

## 1. INTRODUCTION

The task of controlling bipedal robot is often a precarious balance between maintaining formal stability guarantees and expanding control capabilities. This duality has been present since the genesis of bipedal control. Beginning in the 1960's, Zero Moment Point [29] methods were the original foundation of formal biped control, but its validity required significant restrictions on the dynamics of the robot (fully-actuated flat-footed contact). In contrast, the

\*This research is supported by NSF CPS Grant CNS-1239055 and NRI Grant IIS-1526519.

Permission to make digital or hard copies of all or part of this work for personal or classroom use is granted without fee provided that copies are not made or distributed for profit or commercial advantage and that copies bear this notice and the full citation on the first page. Copyrights for components of this work owned by others than ACM must be honored. Abstracting with credit is permitted. To copy otherwise, or republish, to post on servers or to redistribute to lists, requires prior specific permission and/or a fee. Request permissions from [permissions@acm.org](mailto:permissions@acm.org).

HSCC'17, April 18-20, 2017, Pittsburgh, PA, USA

© 2017 ACM. ISBN 978-1-4503-4590-3/17/04...\$15.00

DOI: <http://dx.doi.org/10.1145/3049797.3049823>

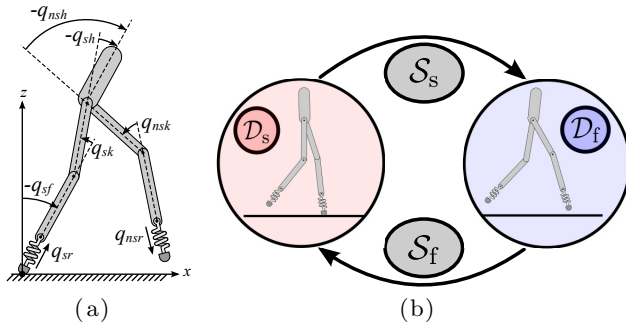


Figure 2: (a) The model of DURUS-2D with two linear springs; (b) The directed cycle structure of the multi-domain hybrid system model for DURUS-2D running.

Raibert hoppers [22] exhibited agile bounces and flips that remain impressive today. But their control was built without the *a priori* confidence of formal methods. Research over the following decades has considerably narrowed this formality gap, with formal approaches rising to the challenge of underactuation [18, 21, 27, 12] and highly dynamic robots incorporating formal analysis in their control [7, 24].

Bipedal robotic running, despite the 30 years that have passed since the Raibert’s hopper, remains an extremely difficult control problem. Very few control methodologies have been presented that lead to experimental success with prominent aerial phases [28, 22, 27]. With an eye toward viewing bipedal running as a hybrid dynamical system: an alternating sequence of stance and flight domains with instantaneous impacts in between, the notion of hybrid zero dynamics (HZD) was used in [10, 5, 19].

HZD operates on a principle of dimensional reduction, aimed at simplifying the numerous degrees of freedom present in legged machines, while also allowing for underactuation. This framework was used to enable bipedal running on MABEL [27], a pivotal demonstration showing the intersection of theory and experiment. However, on top of the HZD framework used on MABEL, there are also important expert-driven adjustments to the implementation, like tuning of control loops, adding feedforward trajectories, and on-line parameter update routines. One way to interpret this is: the gap between the assumed model and the experimental testbed necessitated modifications in the control implementation that is needed to realize stable robotic running. Similar modifications have been used previously for robotic walking implementations [20, 26, 14]. We seek to further reduce the need for this expert adjustment with formal stabilizing controllers.

There are two main central principles underlying our approach: a) gait synthesis via an optimization method, b) controller design that yields formal guarantees of robustness. We use a direct collocation based optimization method coupled with HZD constraints to generate running gaits on the spring-legged robot, DURUS-2D (Fig. 1). This nonlinear programming is notably fast, capable of generating a feasible running gait within a minute that satisfies all physical limitations of the running dynamics. However, the resulting gait that was built upon an ideal model and precise sensing cannot guarantee experimental realization. Unlike theoretical simulation, where most variables are either measurable or exclusively solvable, real world experiments suffer from a

wide array of uncertainties. Indeed, uncertainties like unmodeled dynamics, nonlinear stiffness properties, damping effects and actuators, poor signal to noise ratio, and even deformations due to impacts are often observed. Therefore, we not only seek a fast optimization approach that yields feasible solutions under the assumed model, but also seek a controller formally guaranteeing robustness under real-world constraints. In this paper, we use the notion of *input to state stability* (ISS) that captures the practical limitations of the actuator inputs in an elegant manner. Specifically we address the *phase* based uncertainty that are typically a high deterrence in tracking parameterized functions. Similar problems involving inaccurate phase determinations were solved in [16], where pure time based parameterizations were used. But this paper will construct time+state based parameterizations to yield stronger stability conditions. Note that, in order to realize running, a variety of uncertainties need to be considered. So we will use the solutions from [15, 6] to account for the remaining uncertainties.

The paper is structured as follows. Section 2 introduces the HZD framework in the context of running, and the direct collocation based optimization method to generate running gaits (outputs). Next, Section 3 introduces a state+time based controller for driving these outputs to zero. By using the notion of ISS criterion for hybrid systems, we establish ultimate boundedness and also realize robust variants of the controller [16]. Finally in Section 4, 5, an experimental implementation is explained in detail, together with some simulated results where similar uncertainty was added to the model. The result is a stable, sustainable and agile running on DURUS-2D at 1.75 m/s, with a notable ground clearance and 60% aerial phase. We believe that this successful hardware implementation, which matches simulation results, indicates an important step toward bridging the gap between theory and experiment.

## 2. HZD GAIT GENERATION

In this section, we will introduce the hybrid model of the bipedal running robot, DURUS-2D (Fig. 1). This is the planar version of the three-dimensional DURUS humanoid robot designed and built by SRI International with the objective of achieving dynamic multi-domain underactuated locomotion [13, 9] with special emphasis on energy efficiency. But in the context of running, we will take our first step by investigating the characteristics of 2D robots.

### 2.1 Hybrid Model of Running

**Model Configuration.** As shown in Fig. 2a, the configuration space  $\mathbb{Q} \subset \mathbb{R}^n$ ,  $n = 9$ , of DURUS-2D is defined as  $q = (sf_x, sf_z, \theta_{sf}, r_{sp}, \theta_{sk}, \theta_{sh}, \theta_{nsh}, \theta_{nsk}, r_{nsp})^T \in \mathbb{Q}$ , where  $sf_x$  and  $sf_z$  are the positions of the end points of the stance foot along  $x$  and  $z$  directions,  $r_{sp}, r_{nsp}$  are the deflections of the springs on stance and nonstance legs,  $\theta_{\square}$  are the joint angles of the stance foot, stance knee, stance hip, nonstance hip and nonstance knee. In addition, the control inputs are defined as  $u = (u_{sk}, u_{sh}, u_{nsh}, u_{nsk})^T \in \mathbb{R}^k$ ,  $k = 4$ , which represent the torque applied at knee and hip joints.

**Hybrid System Model.** Bipedal robotic running is represented by a special class of hybrid systems: systems with impulse effects. They can be represented by a tuple:

$$\mathcal{H} = (\mathcal{D}, S, U, \Delta, \mathcal{FG}).$$

Here,  $\mathcal{D} = \{\mathcal{D}_s, \mathcal{D}_f\}$  is the set of domains which are the

sets of possible states assumed by the robot. For running, we have the stance domain  $\mathcal{D}_s$ , where only stance foot is on the ground; and the flight domain  $\mathcal{D}_f$ , where both feet are swinging in the air (see Fig. 2b). The set of guards  $S = \{S_s, S_f\}$  represent the switching surfaces, which are states of the robot at transition. Possible guards are the transition from stance to flight domain:  $S_s$ , and the transition from flight to stance domain:  $S_f$ . Besides,  $\mathcal{U}$  is the set of admissible inputs,  $\Delta$  is the set of switching functions, called impact maps and finally  $\mathcal{FG}$  is the set of fields yielding the continuous dynamics. A mathematical representation of the hybrid system in terms of output dynamics will be given in Section 3.3.

**Continuous Dynamics.** The Equation of Motion (EOM) over a continuous domain  $\mathcal{D}_v$ ,  $v \in \{s, f\}$ , is determined by the Euler-Lagrange equation and holonomic constraints [11]:

$$\begin{aligned} D(q)\ddot{q} + H(q, \dot{q}) &= Bu + J_v^T(q)F_v, \\ J_v(q)\dot{q} + \dot{J}_v(q, \dot{q})\dot{q} &= 0, \end{aligned} \quad (1)$$

where  $D(q) \in \mathbb{R}^{n \times n}$  is the inertia matrix,  $H(q, \dot{q}) \in \mathbb{R}^n$  contains the Coriolis-centrifugal and gravity terms,  $B \in \mathbb{R}^{n \times k}$  is the actuation distribution matrix,  $J_v(q) \in \mathbb{R}^{n \times m}$  is the Jacobian of the holonomic constraints  $\Gamma_v(q)$ , and  $F_v \in \mathbb{R}^m$  is a *wrench* containing the constraint forces or moments, which can be explicitly solved as a function of system states and inputs. The holonomic constraints for each domain are defined as

$$\begin{aligned} \Gamma_s(q) &= (sf_x, sf_z, r_{nsp})^T \\ \Gamma_f(q) &= (r_{sp}, r_{nsp})^T, \end{aligned} \quad (2)$$

meaning, the stance foot must remain on the ground during the stance domain, and stance and nonstance springs must be locked during the flight domain. More details about constrained dynamics can be found in [11]. Further, by defining  $x = (q, \dot{q}) \in \mathbb{R}^{2n}$ , the EOM can be converted to an affine control system:

$$\dot{x} = f_v(x) + g_v(x)u. \quad (3)$$

**Discrete Dynamics.** Because of the landing impact at the end of flight domain  $S_f$ , and the hard stop to prevent stance spring from further oscillation at the end of stance domain  $S_s$ , discrete dynamics are considered (see Fig. 2b). The discrete dynamics are determined by changes in the contact points of the system, for which only the velocity terms are affected through the plastic impacts by imposing the holonomic constraints of the subsequent domain. And the roles of the “stance” and “nonstance” legs are simultaneously swapped. Similar dynamics were detailed for walking in [4].

## 2.2 HZD control Framework

**Virtual Constraints (Outputs).** Any applicable state-based feedback controllers that have been applied on the control system, yield a closed-loop hybrid system [5]. This can be done by defining a set of outputs and applying feedback controllers to drive them to zero. In other words, we define the outputs (also often refereed to as the virtual constraints [20]) of the system on a domain  $\mathcal{D}_v$ ,  $v \in \{s, f\}$  as

$$y_v(q) = y^a(q) - y_v^d(\tau_v), \quad (4)$$

where  $y^a : \mathbb{Q} \rightarrow \mathbb{R}^k$  is the actual output of the system. Here,

it is chosen as the four actuated joint angles:

$$y^a(q) = [\theta_{sk} \ \theta_{sh} \ \theta_{nsh} \ \theta_{nsk}]. \quad (5)$$

And  $y_v^d : \mathbb{R}_{\geq 0} \rightarrow \mathbb{R}^k$  is the desired output represented by a set of 5<sup>th</sup> order Bézier curves  $y_v^d = \mathcal{B}(\alpha_v, \tau_v)$  (the parameters  $\alpha_v$  are solved by an optimization in Section 2.3). The *phase variable*  $\tau_v$  is used to modulates the desired outputs  $y_v^d$ . Normally, in order to make the outputs purely state based, we can have the phase variable  $\tau_v : \mathbb{Q} \rightarrow \mathbb{R}_{\geq 0}$ , purely a function of the robot configuration:

$$\tau_v(q) = \frac{\theta_{sf} - p_v^+}{p_v^- - p_v^+}, \quad (6)$$

with  $p_v^-, p_v^+$  the initial and final position of  $\theta_{sf}$  for  $\mathcal{D}_v$ . Although, it must be noted that state based modulation has implementation difficulties due to noisy sensing of under-actuated degrees of freedom of DURUS-2D. This motivates the use of a time based phase variable  $\tau_v : \mathbb{R}_{\geq 0} \rightarrow \mathbb{R}_{\geq 0}$ ,

$$\tau_v(t) = \sum_{i=0}^5 p_i t^i,$$

where  $p_i$  is a set of power series polynomial coefficients obtained by a curve fitting from  $\tau_v(q)$  w.r.t. time. This has desirable stability properties under sensory perturbations, which will be discussed in Section 3.

**State-Based Feedback Controller.** To drive the virtual constraints (outputs)  $y_v \rightarrow 0$  exponentially for each domain  $\mathcal{D}_v$ , we utilize the feedback linearization control law [3]:

$$u_v = (\mathcal{L}_g \mathcal{L}_f y_v)^{-1} (-\mathcal{L}_f^2 y_v + \mu_v), \quad (7)$$

with  $\mathcal{L}$  the Lie derivative. Applying this control law yields the output dynamics  $\ddot{y}_v = \mu_v$ . Further, by picking  $\mu_v$  as

$$\mu_v = -\frac{2}{\varepsilon} \dot{y}_v - \frac{1}{\varepsilon^2} y_v, \quad 0 < \varepsilon < 1, \quad (8)$$

the virtual constraints will converge to zero exponentially at the rate  $1/\varepsilon > 0$ . Since the number of virtual constraints is less than the degrees of freedom of the robot, the uncontrolled states evolve according to the *zero dynamics*. In other words, we have a set of states defined by the vector:  $\eta_v = [y_v, \dot{y}_v]^T \in \mathbb{R}^{2k}$ , that are controllable, and the set of states defined by  $z_v$ , that are uncontrollable and normal to  $\eta_v$  for each domain  $\mathcal{D}_v$ . We can then reformulate (1) to the following form:

$$\begin{aligned} \dot{\eta}_v &= \underbrace{\begin{bmatrix} 0_{k \times k} & 1_{k \times k} \\ 0_{k \times k} & 0_{k \times k} \end{bmatrix}}_F \eta_v + \underbrace{\begin{bmatrix} 0_{k \times k} \\ 1_{k \times k} \end{bmatrix}}_G \mu_v \\ \dot{z}_v &= \Psi_v(\eta_v, z_v), \end{aligned} \quad (9)$$

where  $\Psi_v$  is assumed Lipschitz continuous. The convergence of the outputs  $\eta_v$  can be shown in terms of Lyapunov functions:  $V_\varepsilon(\eta_v) = \eta_v^T P_\varepsilon \eta_v$ , where  $P_\varepsilon$  is the solution to the *continuous time algebraic Riccati equation* (CARE) (see [3]). By choosing  $\mu_v(\eta)$  from (8), we have  $\dot{V}_\varepsilon \leq -\frac{\gamma}{\varepsilon} V_\varepsilon$  with  $\gamma$  the constant obtained from the CARE. Note that in order to make DURUS-2D run experimentally, a time-based feedback controller is ultimately deployed, which will be explained in Section 3.

**Hybrid Zero Dynamics.** Given the control law (8), the controllable states  $\eta_v$  are driven exponentially to zero. In other words, the control law (7) renders the *zero dynamics surface* exponentially stable and invariant over both continuous domains [5]. However, due to the impact dynamics at

the end of each domain, the invariance of the zero dynamics surface is not guaranteed. Therefore, the goal is to find a set of parameters  $\alpha = \{\alpha_s, \alpha_f\}$ , which defines the desired outputs (4), to ensure there exists a periodic orbit and the zero dynamics surface

$$Z_v = \{(q, \dot{q}) \in \mathcal{D}_v : y_v(q) = 0, \dot{y}_v(q, \dot{q}) = 0\}, \quad v \in \{s, f\},$$

is invariant through impacts, i.e., hybrid invariant. Mathematically, hybrid invariance is represented as

$$\begin{aligned} \Delta(Z_s \cap S_s) &\subset Z_f, \\ \Delta(Z_f \cap S_f) &\subset Z_s. \end{aligned} \quad (10)$$

The process of finding  $\alpha$  is often formulated as a nonlinear constrained optimization problem subject to the multi-domain hybrid system model. Details about the construction of HZD on walking robots can be found in [5].

### 2.3 Direct Collocated Gait Optimization

Once a hybrid control model is defined, a periodic running gait that can be implemented on DURUS-2D is needed. For this purpose, an optimization algorithm is utilized to determine the parameters  $\alpha$  that guarantee HZD. Traditionally, *direct shooting methods* based nonlinear programming (NLP) is often used in bipedal walking [23, 5, 26, 30] and even planar running [31, 27]. However, its key methodology—numerical integration—has made it computationally expensive to solve for a running gait, due to the multiple degrees of underactuation involved in the multi-domain hybrid system. Therefore a *direct collocation method* based NLP is used under the HZD framework. Previously, this method has been applied to the humanoid DURUS to successfully achieve walking [12]. And an extensive study about this NLP on simulated 3D running is detailed in [17].

Essentially, we discretized each continuous domain  $\mathcal{D}_v$  based on time  $t_v^i$ , where  $i = 1, 2, \dots, N$  is defined as the grid index. Let  $x^i$  and  $\dot{x}^i$  be the approximate states and its derivative at node  $i$ , the *defect constraints* at each odd node are defined as

$$\begin{aligned} \dot{x}^i - 3(x^{i+1} - x^{i-1})/2\Delta t_v^i + (\dot{x}^{i-1} + \dot{x}^{i+1})/4 &= 0, \\ x^i - (x^{i+1} - x^{i-1})/2\Delta t_v^i + \Delta t_v^i(\dot{x}^{i-1} + \dot{x}^{i+1})/8 &= 0, \end{aligned}$$

where  $\Delta t_v^i = t_v^{i+1} - t_v^{i-1}$ . Plus,  $x^i, \dot{x}^i$  need to satisfy the dynamical constraints  $\dot{x}^i = f_v(x^i) + g_v(x^i)u^i$ , where  $u^i$  is exclusively solved by (7). In summary, the nonlinear dynamics are treated as an equality constraint with the use of implicit Runge-Kutta methods and *defect variables*. This modification also allows the analytical Jacobians of all optimization constraints to be pre-computed, which dramatically scales down the computation cost. This can also significantly increase the possibilities of finding a feasible solution to the nonlinear system.

Finally, the direct collocation based, constrained optimization can be stated as:

$$\mathcal{Z}^* = \underset{\mathcal{Z}}{\operatorname{argmin}} \sum_{v \in \{s, f\}} J_v(\mathcal{Z}_v) \quad (11)$$

$$\text{s.t. } \mathcal{Z}_{\min} \leq \mathcal{Z}_v \leq \mathcal{Z}_{\max}, \quad (12)$$

$$\mathbf{C}_{\min} \leq \mathbf{C}(\mathcal{Z}_v) \leq \mathbf{C}_{\max}, \quad (13)$$

where  $\mathcal{Z}_v$  is the set of all unknowns including the parameters  $\alpha$  that define the running gait,  $J_v(\mathcal{Z}_v)$  is the objective function which minimizes the torque inputs. And  $\mathbf{C}(\mathcal{Z})$  is a

collection of necessary constraints, such as HZD constraints in (10). A major difference between walking and running, the foot clearance constraint for the flight domain, needs to be enforced on both feet to ensure the robot is in the air. More details about constructing other physical and geometric constraints can be found at [17]. By utilizing this NLP, we are able to generate a HZD running gait within 43 s from an initial guess at  $\mathbf{0}$ , whereas a direct shooting method could require hours of computation [31].

## 3. TIME BASED FEEDBACK

By using the feedback control law given by (7), (8), it can be shown that with sufficiently small  $\varepsilon$ , the output dynamics are exponentially driven to zero. In fact, [3] shows that by picking a *rapidly exponentially stable control Lyapunov function* (RES-CLF), locally exponentially stable hybrid periodic orbits can be realized. However in reality, due to the difficulty in estimating the phase variable (6) (which is a function of the unactuated degrees of freedom), a better controller is required that is less susceptible to the noisy state estimation. Motivated by the time based implementation of the tracking controller in [16], the goal of this section is to construct a controller that uses a time based instead of state based desired trajectory for robotic running.

### 3.1 Input to State Stability

**Feedback Linearization for Time Based Outputs.** For the ease of notations, we will omit the domain representations (the subscripts  $v$ ) in this section. If the state based desired relative degree two outputs are functions of  $q, y^d : \mathbb{Q} \rightarrow \mathbb{R}^k$ , then the time based desired outputs are functions of time  $y^{t,d} : \mathbb{R}_{\geq 0} \rightarrow \mathbb{R}^k$ . We thus have the time based output representation as follows:

$$y^t(t, q) = y^a(q) - y^{t,d}(\tau(t)). \quad (14)$$

Similar to the construction of state based controller (7), we would drive  $y^t \rightarrow 0$  exponentially. Therefore, the feedback controller that linearizes the time based output is given as

$$u_t = (\mathcal{L}_g \mathcal{L}_f y^a)^{-1} \left( -\mathcal{L}_f^2 y^a + \dot{y}^{t,d} + \mu_t \right), \quad (15)$$

where  $\mu_t$  is the linear feedback applied after the feedback linearization. We can either pick  $\mu_t$  via a simple PD law

$$\mu_t = -\frac{2}{\varepsilon} \dot{y}^t - \frac{1}{\varepsilon^2} y^t, \quad (16)$$

for some  $0 < \varepsilon < 1$ , or via an optimal control law through *control Lyapunov functions* (CLFs). Nevertheless, using the time based feedback linearizing controller (15) reduces the nonlinear system (3) to the normal form

$$\begin{aligned} \dot{\eta}_t &= \underbrace{\begin{bmatrix} 0_{k \times k} & 1_{k \times k} \\ 0_{k \times k} & 0_{k \times k} \end{bmatrix}}_F \eta_t + \underbrace{\begin{bmatrix} 0_{k \times k} \\ 1_{k \times k} \end{bmatrix}}_G \mu_t \\ \dot{z}_t &= \Psi_t(\eta_t, z_t), \end{aligned} \quad (17)$$

which is similar to (9), but with the use of time based outputs:  $\eta_t = [y^t, \dot{y}^t]^T \in \mathbb{R}^{2k}$ . Note that the zero dynamics coordinates  $z_t$ , evolve based on time due to the dependency on  $\eta_t$ . Accordingly, if the time based transverse dynamics  $\eta_t$  are 0, we have the zero dynamics  $\dot{z}_t = \Psi_t(0, z_t)$ . Convergence of the time based outputs can be ensured by picking an appropriate time based control law (16). But this controller does not necessarily ensure the convergence of the

state based outputs. We are interested in the stability of the state based transverse dynamics ( $\eta$ ), given that the time based control law is implemented on the robot.

**State based vs. time based control laws.** Given the controller (16) that could drive the time based outputs  $\eta_t \rightarrow 0$ , we will study the evolution of the state based outputs  $\eta$  in (9). By the assumption of Theorem 1 in [3], the controller yields an exponentially stable periodic orbit for hybrid dynamics. Therefore, we will obtain conditions for the stability of this hybrid periodic orbit when a time based control law is applied. Picking the input (15) on the dynamics of state based output  $y$ , we have

$$\ddot{y} = \mathcal{L}_f^2 y + \mathcal{L}_g \mathcal{L}_f y u_t, \quad (18)$$

$$\ddot{y} = \underbrace{\mathcal{L}_f^2 y + \mathcal{L}_g \mathcal{L}_f y u}_{=\mu} + \underbrace{\mathcal{L}_g \mathcal{L}_f y (u_t - u)}_{=:d}, \quad (19)$$

$$\ddot{y} = \mu + d, \quad (20)$$

where  $d = \mathcal{L}_g \mathcal{L}_f y (\mathcal{L}_g \mathcal{L}_f y^a)^{-1} (-\mathcal{L}_f^2 y^a + \ddot{y}^{t,d} + \mu_t) - \mu + \mathcal{L}_f^2 y$ , is obtained by substituting for  $u_t, u$  from (7), (15). An alternative interpretation of (18) is that, the stabilizing control input  $\mu(\eta)$  (which is state based) should have been applied, but instead, the time based input  $\mu + d$  was applied to the state based output dynamics of  $y$ . Applying a time based feedback control law completely eliminated the dependency on the noisy phase variable  $\tau(q)$ , but the consequence is the appearance of the disturbance input  $d$ . The expression for  $d$  can be further simplified to

$$d(t, q, \dot{q}, \ddot{q}, \mu_t, \mu) = (\mu_t - \mu) + (\ddot{y}^{t,d} - \ddot{y}^d). \quad (21)$$

We know that,  $y^d = y^d(\tau(q))$  (for bipedal robots), and it can be observed that  $d$  becomes small by minimizing the error  $\ddot{y}^{t,d}(\tau(t)) - \ddot{y}^d(\tau(q))$ . Therefore  $d$  can be termed *time-phase uncertainty*, or just *phase uncertainty*.

In the context of linear systems, it is important to have bounded state based output dynamics if  $d$  is bounded. Of course, the time based outputs  $\eta_t \rightarrow 0$ . Denote the supremum of the uncertainty over time as  $\|d\|_\infty$ , we can easily establish that a bounded  $d$  results in bounded outputs  $y, \dot{y}$  (or just  $\eta$ ), for the continuous dynamics. However, due to the impact dynamics that are not just nonlinear, but also extremely destabilizing (the noisy impacts can be observed in the video [1]), output boundedness cannot be guaranteed for the hybrid dynamics. This motivates using the notion of input to state stability to establish boundedness on the state based outputs for bipedal robotic running on DURUS-2D.

Going back to (18), we can substitute this formulation in (9), which results in the following representation:

$$\begin{aligned} \dot{\eta} &= F\eta + G\mu + Gd, \\ \dot{z} &= \Psi(\eta, z). \end{aligned} \quad (22)$$

As mentioned before, we are free to pick  $\mu(\eta)$  (say (8)), since the actual control input applied is time based  $\mu_t(\eta_t)$  (from (36)) which is implicit in  $d$ . From the point of view of the state based outputs  $\eta$ , we have the following representation dynamics of the Lyapunov function:

$$\dot{V}_\varepsilon = \eta^T (F^T P_\varepsilon + P_\varepsilon F)\eta + 2\eta^T P_\varepsilon G\mu + 2\eta^T P_\varepsilon Gd, \quad (23)$$

obtained by substituting (22) for  $\eta$ . Using the linear feedback law  $\mu(\eta)$  from (8), the following is obtained:

$$\dot{V}_\varepsilon \leq -\frac{\gamma}{\varepsilon} V_\varepsilon + 2\eta^T P_\varepsilon Gd. \quad (24)$$

It should be noted that even though the time based controller leads to convergence of time based outputs  $y^t \rightarrow 0$ , equation (24) extends it to state based outputs  $y$  that are driven exponentially to an ultimate bound. And this ultimate exponential bound is explicitly derived from  $d$ , which is established via the notion of *input to state stability* (ISS).

**Input to State Stability.** We will first introduce the basic definitions and results related to ISS for a general nonlinear system and then focus on the hybrid running dynamics (see [25] for a detail survey on ISS). Assume we have a general nonlinear system, represented in the following fashion:

$$\dot{x} = f(x, d), \quad (25)$$

with  $x$  taking values in Euclidean space  $\mathbb{R}^n$ , the input  $d \in \mathbb{R}^m$  for some positive integers  $n, m$ . The mapping  $f : \mathbb{R}^n \times \mathbb{R}^m \rightarrow \mathbb{R}^n$  is considered Lipschitz continuous and  $f(0, 0) = 0$ . It can be seen that the input considered here is  $d$ . Therefore, the construction is such that a stabilizing controller  $u(x)$  has been applied (such as (7)). Any deviation from this stabilizing controller can be viewed as  $u(x) + d$ , with  $d$  being a new disturbance input. In the example of the linearized system (22), a suitable stabilizing controller  $\mu(\eta)$  is applied and the effect of the disturbance input  $d$  is analyzed. We assume that  $d$  takes values in the space of all Lebesgue measurable functions:  $\|d\|_\infty = \text{ess.sup}_{t \geq 0} \|d(t)\| < \infty$ , which can be denoted as  $d \in \mathbb{L}^\infty$ .

**Class  $\mathcal{K}_\infty$  and  $\mathcal{KL}$  functions.** A class  $\mathcal{K}_\infty$  function is a function  $\alpha : \mathbb{R}_{\geq 0} \rightarrow \mathbb{R}_{\geq 0}$  which is continuous, strictly increasing, unbounded, and satisfies  $\alpha(0) = 0$ . And a class  $\mathcal{KL}$  function is a function  $\beta : \mathbb{R}_{\geq 0} \times \mathbb{R}_{\geq 0} \rightarrow \mathbb{R}_{\geq 0}$  such that  $\beta(r, \cdot) \in \mathcal{K}_\infty$  for each  $t$  and  $\beta(\cdot, t) \rightarrow 0$  as  $t \rightarrow \infty$ .

We can now define ISS for the system (25).

**Definition 1.** *The system (25) is input to state stable (ISS) if there exists  $\beta \in \mathcal{KL}$ ,  $\iota \in \mathcal{K}_\infty$  such that*

$$|x(t, x_0)| \leq \beta(|x_0|, t) + \iota(\|d\|_\infty), \quad \forall x_0, \forall t \geq 0, \quad (26)$$

and considered locally ISS, if the inequality (26) is valid for an open ball of radius  $r$ ,  $x_0 \in \mathbb{B}_r(0)$ .

**Definition 2.** *The system (25) is exponentially input to state stable (e-ISS) if there exists  $\beta \in \mathcal{KL}$ ,  $\iota \in \mathcal{K}_\infty$  and a positive constant  $\lambda > 0$  such that*

$$|x(t, x_0)| \leq \beta(|x_0|, t)e^{-\lambda t} + \iota(\|d\|_\infty), \quad \forall x_0, \forall t \geq 0, \quad (27)$$

and considered locally e-ISS, if the inequality (27) is valid for an open ball of radius  $r$ ,  $x_0 \in B_r(0)$ .

**ISS-Lyapunov functions.** We can develop Lyapunov functions that satisfy the ISS conditions and achieve the stability property.

**Definition 3.** *A smooth function  $V : \mathbb{R}^n \rightarrow \mathbb{R}_{\geq 0}$  is an ISS-Lyapunov function for (25) if there exist functions  $\underline{\alpha}$ ,  $\bar{\alpha}$ ,  $\alpha$ ,  $\iota \in \mathcal{K}_\infty$  such that*

$$\begin{aligned} \underline{\alpha}(|x|) &\leq V(x) \leq \bar{\alpha}(|x|) \\ \dot{V}(x, d) &\leq -\alpha(|x|) \quad \text{for } |x| \geq \iota(\|d\|_\infty). \end{aligned} \quad (28)$$

The following lemma establishes the relationship between the ISS-Lyapunov function and the ISS of (25).

**Lemma 1.** *The system (25) is ISS if and only if it admits a smooth ISS-Lyapunov function.*

Proof of Lemma 1 was given in [25]. In fact the inequality condition can be made stricter by using the exponential estimate:

$$\dot{V}(x, d) \leq -cV(x) + \iota(\|d\|_\infty), \quad \forall x, d. \quad (29)$$

which is then called the e-ISS Lyapunov function.

### 3.2 Phase Uncertainty to State Stability

We can now define the notion of *phase to state stability* (PSS). Without loss of generality, we denote  $(\eta, z) = (\eta_v, z_v)$ , and the subscript  $v$  will be specified when a specific domain (s or f) is considered.

**Definition 4.** Assume a ball of radius  $r$  centered at the origin. The system given by (22) is locally *phase to  $\eta$  stable*, if there exists  $\beta \in \mathcal{KL}$ ,  $\iota \in \mathcal{K}_\infty$  such that

$$|\eta(t)| \leq \beta(|\eta(0)|, t) + \iota(\|d\|_\infty), \forall \eta(0) \in \mathbb{B}_r(0), \forall t \geq 0, \quad (30)$$

and it is locally PSS if

$$|(\eta(t), z(t))| \leq \beta(|(\eta(0), z(0))|, t) + \iota(\|d\|_\infty), \quad \forall \eta(0) \in \mathbb{B}_r(0), \forall t \geq 0.$$

Based on the asymptotic gain and zero stability property of the system (22) w.r.t. the *phase uncertainty*  $d$ , we have the following lemma.

**Lemma 2.** Given the controller  $\mu(\eta)$  in (8), the system (22) is *phase to  $\eta$  stable*.

PROOF. Based on the constructions of the Lyapunov function  $V_\varepsilon$ , we have the dynamics of the from (24):

$$\begin{aligned} \dot{V}_\varepsilon &\leq -\frac{\gamma}{\varepsilon} V_\varepsilon + 2\eta^T P_\varepsilon G d \\ &\leq -\frac{\gamma}{\varepsilon} V_\varepsilon + 2\|\eta\| \|P_\varepsilon\| \|d\|_\infty \\ &\leq -\frac{\gamma}{2\varepsilon} V_\varepsilon \quad \text{for } |\eta| \geq \frac{4c_2}{\gamma c_1 \varepsilon} \|d\|_\infty, \end{aligned} \quad (31)$$

which is thus an ISS-Lyapunov function (28).  $\square$

We can also realize exponentially ultimate boundedness of the entire dynamics by appending a state based linear feedback law to the time based feedback controller (16)

$$u_T = u_t + \bar{\mu}, \quad (32)$$

which results in the following output dynamics in the place of (18):

$$\ddot{y} = \mu + d + \mathcal{L}_g \mathcal{L}_f y \bar{\mu}. \quad (33)$$

$\mathcal{L}_g \mathcal{L}_f y$  can be explicitly computed as  $\mathcal{L}_g \mathcal{L}_f y = \mathcal{J} D^{-1} B$ , where  $D$  and  $B$  are obtained from (1), and  $\mathcal{J} = \partial y / \partial q$  is the Jacobian of the outputs. Since  $D$  is invertible, it can be easily shown that  $\mathcal{J} D^{-1} B$  is invertible. By applying (32), system (22) will have an extra input  $\bar{\mu}$  that yields:

$$\begin{aligned} \dot{\eta} &= F\eta + G\mu + Gd + G\mathcal{J}D^{-1}B\bar{\mu} \\ \dot{z} &= \Psi(\eta, z), \end{aligned} \quad (34)$$

then (24) gets reformulated as

$$\dot{V}_\varepsilon \leq -\frac{\gamma}{\varepsilon} V_\varepsilon + 2\eta^T P_\varepsilon G d + 2\eta^T P_\varepsilon G \mathcal{J} D^{-1} B \bar{\mu}. \quad (35)$$

By picking a control law for the auxiliary input

$$\bar{\mu} = -\frac{1}{2\varepsilon} (\mathcal{J} D^{-1} B)^{-1} G^T P_\varepsilon \eta, \quad (36)$$

we have the following simplification of (35):

$$\dot{V}_\varepsilon \leq -\frac{\gamma}{\varepsilon} V_\varepsilon + 2\eta^T P_\varepsilon G d - \frac{1}{\varepsilon} \eta^T P_\varepsilon G G^T P_\varepsilon \eta. \quad (37)$$

Therefore, by defining the semi-definite function  $\bar{V}_\varepsilon(\eta) = \eta^T P_\varepsilon G G^T P_\varepsilon \eta$ , we can pick  $\bar{\varepsilon}$  small enough to cancel the effect of *phase uncertainty* on the dynamics. Lemma 2 can now be redefined to obtain exponential ultimate boundedness for the new control input (32).

**Lemma 3.** Given the controllers  $\mu(\eta)$  in (8), and  $\bar{\mu}(\eta)$  in (36), the system (34) is *exponentially phase to  $\eta$  stable* w.r.t. the input disturbance  $d \in \mathbb{L}^\infty$ .

PROOF. We again pick the derivative of the Lyapunov function  $V_\varepsilon$  resulting in

$$\begin{aligned} \dot{V}_\varepsilon &\leq -\frac{\gamma}{\varepsilon} V_\varepsilon - \frac{1}{\bar{\varepsilon}} \eta^T P_\varepsilon G G^T P_\varepsilon \eta + 2\eta^T P_\varepsilon G d \\ &\leq -\frac{\gamma}{\varepsilon} V_\varepsilon \quad \text{for } |\eta| \geq \frac{2\bar{\varepsilon} c_2}{c_1^2 \varepsilon^2} \|d\|_\infty, \end{aligned} \quad (38)$$

which satisfies the exponential estimate (29).  $\square$

Now Lemma 3 can be extended to include the uncontrolled states  $z$  given that they are stable. Let  $Y \subset \mathbb{R}^{2k}$ ,  $Z \subset \mathbb{R}^{2(n-k)}$ ,  $\phi_t(\eta, z)$  be the flow of (34) with the initial condition  $(\eta, z) \in Y \times Z$ . And let the flow  $\phi_t$  be periodic with period  $T_* > 0$  and a fixed point  $(\eta^*, z^*)$  if  $\phi_{T_*}(\eta^*, z^*) = (\eta^*, z^*)$ . Associated with the periodic flow is the periodic orbit

$$\mathcal{O} = \{\phi_t(\eta^*, z^*) \in Y \times Z : 0 \leq t \leq T_*\}.$$

Similarly, we denote the flow of the zero dynamics given by (34) by  $\phi_t|_z$  and for a periodic flow we denote the corresponding periodic orbit by  $\mathcal{O}_z = \mathcal{O}|_z$ . Due to the invariance of the zero dynamics, we have the mapping  $\iota_0 : \mathcal{O}_z \rightarrow \mathcal{O}$ , where  $\iota_0 : Z \rightarrow Y \times Z$  is the canonical embedding. For any  $(\eta, z)$ , we can denote the distance from  $\mathcal{O}$  as  $\|(\eta, z)\|_{\mathcal{O}}$ . We now have the following theorem to establish *phase to state stability* of  $\mathcal{O}$ .

**Theorem 1.** Assume that the periodic orbit  $\mathcal{O}_z \subset Z$  is *exponentially stable in the zero dynamics*. Given the controllers  $\mu(\eta)$  in (8),  $\bar{\mu}(\eta)$  in (36) applied on (34), that render the outputs *exponential phase to  $\eta$  stable*, then the periodic orbit  $\mathcal{O}$  obtained from the canonical embedding is *exponentially phase to state stable*.

PROOF SKETCH. By the converse Lyapunov theorems, we can construct a quadratic Lyapunov function for the zero dynamics,  $V_z(z)$  that satisfies the exponential inequality constraint:

$$\begin{aligned} c_4 \|z\|_{\mathcal{O}_z}^2 &\leq V_z \leq c_5 \|z\|_{\mathcal{O}_z}^2, \\ \frac{\partial V_z}{\partial z} \Psi(0, z) &\leq -c_6 V_z, \quad \left| \frac{\partial V_z}{\partial z} \right| \leq c_7 \|z\|_{\mathcal{O}_z}, \end{aligned} \quad (39)$$

where  $\|z\|_{\mathcal{O}_z} = \|(0, z)\|_{\mathcal{O}}$ . Consider the following Lyapunov candidate for the full order dynamics:  $V_\varepsilon(\eta, z) = \sigma V_z(z) + V_\varepsilon(\eta)$ . This Lyapunov function is quadratic and satisfies the boundedness properties. Taking the derivative

$$\begin{aligned} \dot{V}_\varepsilon &\leq -\sigma \frac{\partial V_z}{\partial z} \Psi(\eta, z) + \sigma \frac{\partial V_z}{\partial z} (\Psi(\eta, z) - \Psi(0, z)) + \dot{V}_\varepsilon, \\ &\leq -\sigma c_6 V_z + \sigma c_7 L_q \|z\|_{\mathcal{O}_z} \|\eta\| - \frac{\gamma}{\varepsilon} V_\varepsilon, \text{ for } |\eta| \geq \frac{2\bar{\varepsilon} c_2}{c_1^2 \varepsilon^2} \|d\|_\infty, \end{aligned}$$

where the bounds on  $\eta$  are obtained from (38). By picking a suitable  $\sigma$ , we can render  $\dot{V}_\varepsilon$  negative definite.  $\square$

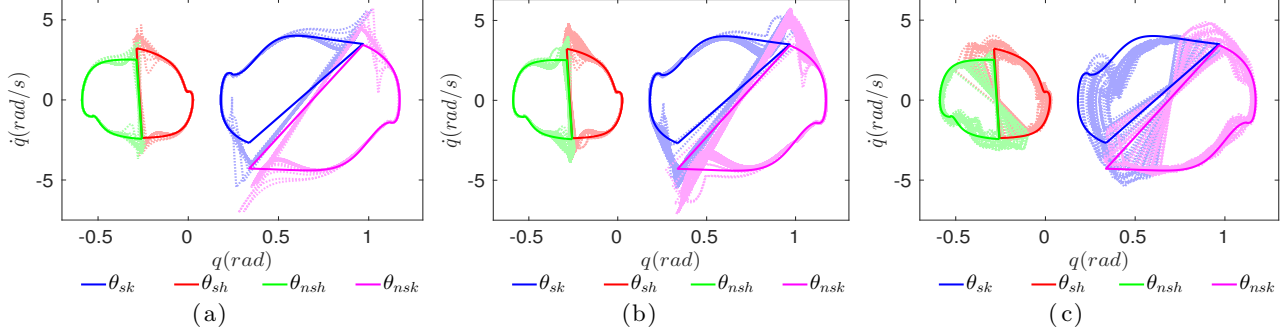


Figure 3: Limit cycles of (a) simulation where time based IO + state based PD controller was applied for 100 steps; (b) Simulation where white noise was added to  $\tau_v(q)$ ; (c) Experimental data. Note the solid lines are the designated gait.

### 3.3 PSS for Hybrid Dynamics

In this part, we can extend the stability properties for hybrid systems. The subscripts  $v$  will be reintroduced to distinguish the domain representations. Here, we define the two-domain hybrid system that represents running dynamics of the robot in the following manner:

$$\mathcal{H} = \begin{cases} \dot{\eta}_v = F\eta_v + G\mu_v + GJD^{-1}B\bar{\mu}_v + Gd \\ \dot{z}_v = \Psi_v(\eta_v, z_v), & \text{if } (\eta_v, z_v) \in \mathcal{D}_v \setminus S_v \\ \eta_f^+ = \Delta_\eta(\eta_s^-, z_s^-) \\ z_f^+ = \Delta_z(\eta_s^-, z_s^-), & \text{if } (\eta_s^-, z_s^-) \in S_s \\ \eta_s^+ = \Delta_\eta(\eta_f^-, z_f^-) \\ z_s^+ = \Delta_z(\eta_f^-, z_f^-), & \text{if } (\eta_f^-, z_f^-) \in S_f \end{cases} \quad (40)$$

where  $\eta = \{\eta_s, \eta_f\}$ ,  $z = \{z_s, z_f\}$ ,  $\mathcal{D}_v$  are the domains and  $S_v$  are the switching surfaces given by

$$\begin{aligned} \mathcal{D}_s &= \{(\eta_s, z_s) \in Y \times Z : h_{nsf} > 0, h_{sf} = 0\}, \\ \mathcal{D}_s &= \{(\eta_s, z_s) \in Y \times Z : h_{nsf} > 0, h_{sf} = 0, \dot{h}_{sf} \geq 0\}, \\ \mathcal{D}_f &= \{(\eta_f, z_f) \in Y \times Z : h_{nsf} \geq 0, h_{sf} > 0\}, \\ \mathcal{D}_f &= \{(\eta_f, z_f) \in Y \times Z : h_{nsf} = 0, h_{sf} > 0, \dot{h}_{nsf} < 0\}, \end{aligned}$$

with  $h_{sf}, h_{nsf} : Y \times Z \rightarrow \mathbb{R}$  the heights of the stance and nonstance foot respectively. The reset map  $\Delta(\eta_v, z_v) = (\Delta_\eta(\eta_v, z_v), \Delta_z(\eta_v, z_v))$  represents the discrete dynamics of the system. For the robot, it represents the impact dynamics of the system when it switches from flight to stance phase and vice versa. Plastic impacts are assumed.

In order to obtain bounds on the output dynamics for hybrid periodic orbits, it is assumed that  $\mathcal{H}$  has hybrid zero dynamics for state based control law given by (7) and (8). More specifically we assume that  $\Delta_\eta(0, z_v) = 0$ , so that the surface  $Z$  is invariant through the discrete dynamics. The hybrid zero dynamics can be described as

$$\mathcal{H}|_Z = \begin{cases} \dot{z}_v = \Psi(0, z_v) & \text{if } z_v \in Z \setminus (S_s \cup S_f) \\ z_f^+ = \Delta_z(0, z_s^-) & \text{if } z_s^- \in (S_s \cap Z) \\ z_s^+ = \Delta_z(0, z_f^-) & \text{if } z_f^- \in (S_f \cap Z). \end{cases} \quad (41)$$

Let  $\phi_t(\eta, z)$  be the hybrid flow of (22) with the initial condition  $(\eta, z)$ ,  $t$  be the time, which is typically the time taken to pass through all domains. Since we are considering a two-domain hybrid system, if  $(\eta, z) \in S_f$ , then  $\phi_t(\eta, z) = \phi_{t_1}^f \circ \Delta \circ \phi_{t_2}^s(\Delta(\eta, z))$ , and  $t = t_1 + t_2$ . The flow  $\phi_t$  is periodic with period  $T > 0$ , and a fixed point  $\phi_T(\eta^*, z^*) = (\eta^*, z^*)$ . For the period  $T$ ,  $T_1, T_2$  are the impact times in the two domains such that  $T_1 + T_2 = T$ . Associated with the periodic

flow is the periodic orbit  $\mathcal{O} = \{\phi_{t_1}^s(\Delta(\eta^*, z^*)) \cup \phi_{t_2}^f \circ \Delta \circ \phi_{T_1}^s(\Delta(\eta^*, z^*)) : 0 \leq t_1 \leq T_1, 0 \leq t_2 \leq T_2\}$ . Similarly, we denote the flow of the zero dynamics  $\dot{z} = \Psi(0, z)$  by  $\phi_T|_Z$  and for a periodic flow we denote the corresponding periodic orbit by  $\mathcal{O}_z \subset Z$ . The periodic orbit in  $Z$  corresponds to a periodic orbit for the full order dynamics,  $\mathcal{O} = \iota_0(\mathcal{O}_z)$ , through the canonical embedding  $\iota_0(z) = (0, z)$ .

**Main Theorem.** We can now introduce the main theorem of the paper. Similar to the continuous dynamics, it is assumed that the periodic orbit  $\mathcal{O}_z$  is exponentially stable in the hybrid zero dynamics.

**Theorem 2.** *Let  $\mathcal{O}_z$  be an exponentially stable periodic orbit of the hybrid zero dynamics  $\mathcal{H}|_Z$  transverse to  $S \cap Z$ . Given the controllers  $\mu_v(\eta_v)$  in (8),  $\bar{\mu}_v(\eta_v)$  in (36), and given  $r > 0$  such that  $(\eta, z) \in \mathbb{B}_r(0, 0)$ , then there exists  $\delta_d > 0$  such that  $\forall \|d\|_\infty < \delta_d$  the periodic orbit  $\mathcal{O}$  is phase to state stable.*

**PROOF SKETCH.** A sketch of the proof is provided here due to space limits. We shall use most of the concepts from [3]. Proof is also similar to that provided for parameter uncertainty in [15]. The key idea is to establish the boundedness of states for a bounded phase uncertainty  $d$ . We just need to realize a discrete time Lyapunov function for a Poincaré map that satisfies the conditions of an ISS-Lyapunov function. Note that for a small enough  $\varepsilon > 0$ , and  $\|d\|_\infty = 0$ , the full order periodic orbit  $\mathcal{O}$  is exponentially stable. For  $\|(\eta, z)\|_{\mathcal{O}} \geq \iota(\|d\|_\infty)$ , we know that with sufficiently small  $\varepsilon$  in (36) we can retain the original convergence rate as indicated by (38). Thus, for the continuous dynamics,  $\dot{V}_\varepsilon \leq -\frac{\gamma}{\varepsilon}V_\varepsilon$  for  $\|(\eta, z)\|_{\mathcal{O}}$  sufficiently large. With this inequality, all of the formulations from equations (61) to (67) in [3] can be used. In other words, the periodic orbit  $\mathcal{O}$  is exponentially converging till the ultimate bound, meaning the periodic orbit  $\mathcal{O}$  is exponentially phase to state stable.  $\square$

Theorem 2 has powerful implications, due to the elimination of the noisy phase variable estimation. This elimination has its effect on tracking, which yields lower errors than that for the noisy phase based modulation. The time based phase modulation is a smooth and better candidate to replicate the unknown actual phase of the robot. This methodology can be easily extended to all kinds of additive uncertainties observed in hybrid systems in general. See [15] for analysis on parameter uncertainty.

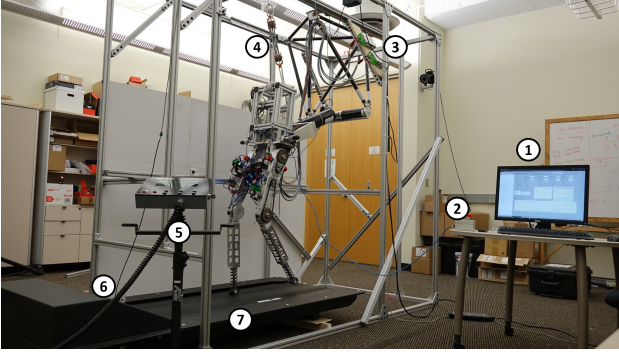


Figure 4: Experimental setup for DURUS-2D running: 1) Control station computer, 2) Emergency stop, 3) Four LiPo batteries, 4) Tripping harness, 5) Treadmill control panel, 6) Encoder Wheel to measure treadmill speed, 7) Treadmill.

## 4. EXPERIMENTAL IMPLEMENTATION

With the optimal running gait generated (Section 2.3) and time dependent RES-CLF controller defined (Section 3.3), we achieved sustainable robotic running. The goal of this section is to describe the experimental setup and the control methods adopted to realize stable running on DURUS-2D.

**DURUS-2D Hardware.** A popular approach for robotic running is to utilize the *spring-loaded inverted pendulum* (SLIP) model [8, 24], where the presence of springs allows for storing energy during high speed impacts thereby improving energy efficiency and torque performance. The previous version of DURUS-2D [9], had rigid carbon fiber calves, unlike the current version which has a linear spring at the end of each aluminum calf. The spring has a stiffness of 20 000 N/m and a damping constant of 100 N s/m. In addition, a 11.5 kg torso is installed to resemble the human weight distribution. The positions and velocities of the torso, knee and hip joints are measured by the attached incremental encoders. Further, the actuated joints, knees and hips, are powered by BLDC motors via cycloidal gear reduction, that provides a maximum continuous torque of 200 N m. With the new legs, DURUS-2D weighs 41.7 kg. Other details about the electrical and software system can be found in [9].

**Experimental Setup.** As shown in Fig. 4, DURUS-2D is mounted on a carbon fiber boom structure which is attached to a cage frame via a fixed one dimensional track. This setup is used to isolate the lateral motions, leaving DURUS-2D to move freely in the sagittal plane. Moreover, the treadmill speed is measured by an encoder wheel and fed to the robot as an environment feedback.

**Switching logic.** Guard condition is used to switch the controller to the subsequent domain (stance or flight). In simulation, the guard condition is triggered when non-stance spring returns to the neutral position for stance domain, i.e.,  $r_{sp} = 0$ . And when the nonstance foot lands on the ground, i.e.,  $nsf_z = 0$ , the flight domain ends. However, due to a lack of effective sensing mechanism, we developed a time+state based switching logic for experiments. For a particular domain  $\mathcal{D}_v$ , the maximum value of time  $t_v^{max}$  and phase variable  $\tau_v^{max}$  can be obtained from the gait design process. Then the guard condition is triggered when  $t > 1.2t_v^{max}$ . But if  $t < 1.2t_v^{max}$ , the guard will be triggered if  $\tau_v(q) > \tau_v^{max}$ . This way, the controller can respond to the

feedback similarly to simulation while allowing for sensing noise of the phase variable.

**Experimental Controller.** Motivated by the results on ISS properties of PD controlled robotic systems in [6], we can replace the time based IO with a time based PD control law, and claim that the resulting system still retains desirable stability properties. For a robot like DURUS-2D, the inertia of the motor (proportional to the square of the gear ratio) coupled with relatively light legs results in stronger ISS conditions for model based uncertainty (see [15, 6]). We therefore pick a time+state based PD control law as follows

$$u_E = -K_p^t y_v^t - K_d^t \dot{y}_v^t - K_p y_v - K_d \dot{y}_v, \quad (42)$$

where  $K_p^t, K_d^t, K_p, K_d$  are constant gain matrices with appropriately tuned values.

## 5. RESULTS

We first validate the proposed control law in simulation. As explained in Section 2, a HZD running gait was first generated that meets all physical limitations, which assumed a feedback linearization controller (7). Then we utilized the time based feedback linearization + state based PD control law given by (32) (see Section 3) in simulation, stable trajectory tracking is achieved that is ultimately bounded to the periodic orbit (see Fig. 7b for the evolution of virtual constraints, i.e., output errors, for 100 steps, and Fig. 3a for phase portrait that is also bounded around the desired gait) when the phase uncertainty is bounded (Fig. 7a). However, in experiments, noisy sensing often occurs around impact dynamics. Therefore to simulate an unideal case, we added a noise signal with amplitude 0.1 to  $\tau_s(q)$  before and after impacts (see Fig. 7c). By applying the same controller, ultimate boundness was also achieved (see Fig. 7d and Fig. 3b) and a stable bipedal running is accomplished. The running tiles are shown in Fig. 5. These simulated results, as a proof of concept, aligned with Theorem 2 in Section 3.3.

In reality, neither state based phase measurements  $\tau_v(q)$ , nor time based phase calculation  $\tau_v(t)$  is capable of producing successful bipedal running (watch [2] for the failed running when pure time based controller was used). However, by applying a variant of time + state based feedback as shown by (42), a sustainable running on DURUS-2D is immediately shown in real world experiments. Multiple views in [1] show that the running is repeatable for over 150 steps. The phase portrait for 30 steps are shown in Fig. 3c, and the output errors are shown in Fig. 7f, both of which have shown ultimate boundedness. Further, the time based and state based phase variables are shown in Fig. 7e. Experimental running tiles are compared to simulation at Fig. 5. The most distinguishable feature of running, foot clearance, is shown in Fig. 6, with the maximum clearance 13 cm, and the flight domain takes 60% of one step. The average running speed is 1.75 m/s, and the measured average mechanical cost of transport (MCOT) for 100 steps is 0.5287.

## 6. CONCLUSIONS

The high degrees of underactuation coupled with rapid switching behaviors between two domains (stance and flight) make bipedal running an important problem, both from a theoretical and experimental standpoint. The success of the demonstrated results serves two important purposes: 1) The reliability and efficiency of the direct collocation based tra-

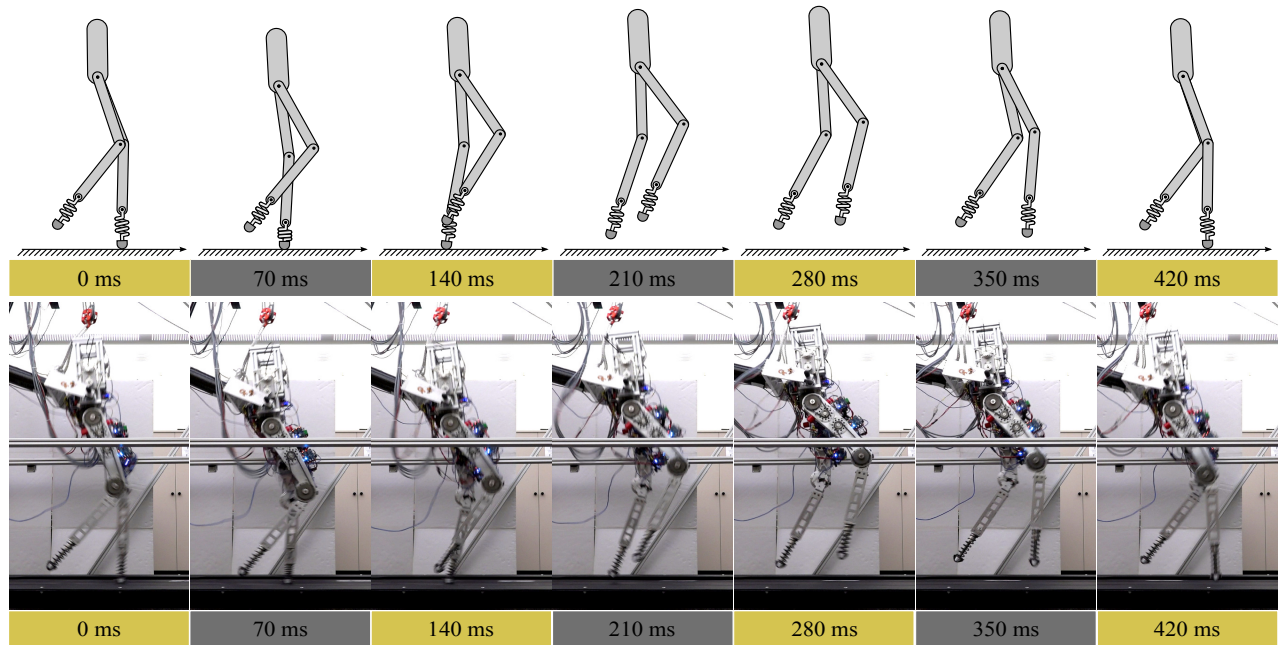


Figure 5: Running tiles of simulation (top) vs. experiment (bottom) for one step.

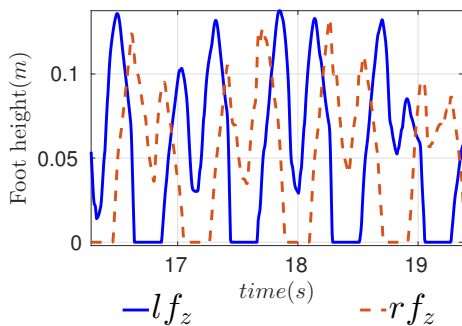


Figure 6: Left and Right Foot Height (ground clearance).

jectory optimization; 2) The ability of the novel phase uncertainty to state stability criterion to construct controllers yielding stability guarantees under sensing uncertainties. In summary, the theoretical framework involving running gait generation and controller design process are shown to predict and produce successful experimental running, taking an important step toward bridging the gap between theory and experiment. Future work will involve expanding on these techniques to realize 3D running.

## 7. REFERENCES

- [1] Bipedal robotic running of DURUS-2D. [https://youtu.be/6k9\\_tf4ctk4](https://youtu.be/6k9_tf4ctk4).
- [2] Failed time based running. <https://youtu.be/2Stq0Q1bEFk>.
- [3] A. Ames, K. Galloway, K. Sreenath, and J. Grizzle. Rapidly exponentially stabilizing control lyapunov functions and hybrid zero dynamics. *Automatic Control, IEEE Transactions on*, 59(4):876–891, 2014.
- [4] A. D. Ames. Human-inspired control of bipedal robots via control lyapunov functions and quadratic programs. In *Proceedings of the 16th international conference on Hybrid systems: computation and control*, pages 31–32. ACM, 2013.
- [5] A. D. Ames. Human-inspired control of bipedal walking robots. *IEEE Transactions on Automatic Control*, 59(5):1115–1130, May 2014.
- [6] D. Angeli. Input-to-state stability of pd-controlled robotic systems. *Automatica*, 35(7):1285 – 1290, 1999.
- [7] P. A. Bhounsule, J. Cortell, A. Grewal, B. Hendriksen, J. D. Karssen, C. Paul, and A. Ruina. Low-bandwidth reflex-based control for lower power walking: 65 km on a single battery charge. *The International Journal of Robotics Research*, 33(10):1305–1321, 2014.
- [8] R. Blickhan. The spring–mass model for running and hopping. *Journal of Biomechanics*, 22(11):1217–1227.
- [9] E. Cousineau and A. D. Ames. Realizing underactuated bipedal walking with torque controllers via the ideal model resolved motion method. In *Robotics and Automation (ICRA), IEEE International Conference on*, pages 5747–5753, May 2015.
- [10] J. W. Grizzle, G. Abba, and F. Plestan. Asymptotically Stable Walking for Biped Robots: Analysis via Systems with Impulse Effects. *IEEE Trans. on Automatic Control*, 46(1):51–64, Jan. 2001.
- [11] J. W. Grizzle, C. Chevallereau, R. W. Sinnet, and A. D. Ames. Models, feedback control, and open problems of 3D bipedal robotic walking. *Automatica*, 50(8):1955 – 1988, 2014.
- [12] A. Hereid, E. Cousineau, C. Hubicki, and A. D. Ames. 3D dynamic walking with underactuated humanoid robots: A direct collocation framework for optimizing hybrid zero dynamics. In *IEEE International Conference on Robotics and Automation*, 2016.
- [13] A. Hereid, C. M. Hubicki, E. A. Cousineau, J. W. Hurst, and A. D. Ames. Hybrid zero dynamics based

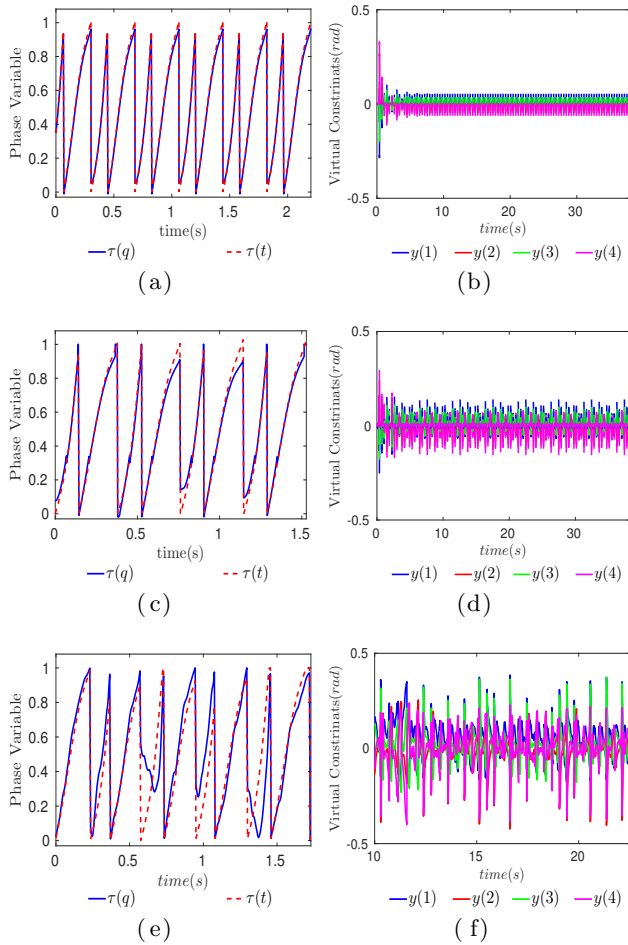


Figure 7: The left column is the phase variables which are used to calculate time and state based outputs:  $y^{d,t}(t) = y_v^d(\tau_v(t))$ ,  $y^d(q) = y_v^d(\tau_v(q))$ , the right column is output errors (virtual constraints) showing ultimate boundedness. (a, b, c, d) are from two simulations with controller given by (32). And (c, d) has a sinusoidal disturbance with 10% amplitude added to  $\tau_v(q)$ ; (e, f) are from experiments.

multiple shooting optimization with applications to robotic walking. In *Robotics and Automation (ICRA), IEEE International Conference on*, 2015.

- [14] S. Kolathaya and A. D. Ames. Achieving bipedal locomotion on rough terrain through human-inspired control. In *Safety, Security, and Rescue Robotics (SSRR), IEEE International Symposium on*, 2012.
- [15] S. Kolathaya and D. A. Ames. Parameter to state stability of control lyapunov functions for hybrid system models of robots. In *Nonlinear Analysis Hybrid Systems*. Elsevier, 2016.
- [16] S. Kolathaya, A. Hereid, and A. D. Ames. Time dependent control lyapunov functions and hybrid zero dynamics for stable robotic locomotion. In *American Control Conference (ACC)*. IEEE, 2016.
- [17] W. Ma, A. Hereid, C. Hubicki, and A. D. Ames. Efficient hzd gait generation for three-dimensional underactuated humanoid running. In *2016 IEEE International Conference on Intelligent Robots and Systems (IROS)*, Korea, 2016.
- [18] I. R. Manchester, U. Mettin, F. Iida, and R. Tedrake. Stable dynamic walking over uneven terrain. *The International Journal of Robotics Research*, 30(3):265–279, Jan. 2011.
- [19] A. E. Martin, D. C. Post, and J. P. Schiedeler. Design and experimental implementation of a hybrid zero dynamics-based controller for planar bipeds with curved feet. *The International Journal of Robotics Research*, 33(7):988–1005, 2014.
- [20] B. Morris and J. Grizzle. Hybrid invariant manifolds in systems with impulse effects with application to periodic locomotion in bipedal robots. *IEEE Transactions on Automatic Control*, 54(8):1751–1764.
- [21] H. Park, K. Sreenath, A. Ramezani, and J. W. Grizzle. Switching control design for accommodating large step-down disturbances in bipedal robot walking. In *IEEE/RSJ International Conference on Robotics and Automation (ICRA)*, pages 45–50. Ieee, May 2012.
- [22] M. Raibert. *Legged robots that balance*, volume 3. MIT press Cambridge, MA, 1986.
- [23] A. V. Rao. A survey of numerical methods for optimal control. *Advances in the Astronautical Sciences*, 2009.
- [24] S. Rezazadeh, C. M. Hubicki, M. Jones, A. Peekema, J. Van Why, A. Abate, and J. Hurst. Spring-mass walking with ATRIAS in 3D: Robust gait control spanning zero to 4.3 kph on a heavily underactuated bipedal robot. In *Proceedings of the ASME 2015 Dynamic Systems and Control Conference*, 2015.
- [25] E. D. Sontag. Input to state stability: Basic concepts and results. In *Nonlinear and optimal control theory*, pages 163–220. Springer, 2008.
- [26] K. Sreenath, H. Park, I. Poulakakis, and J. W. Grizzle. A compliant hybrid zero dynamics controller for stable, efficient and fast bipedal walking on MABEL. *The International Journal of Robotics Research*, 30(9):1170–1193, 2011.
- [27] K. Sreenath, H.-W. Park, I. Poulakakis, and J. Grizzle. Embedding active force control within the compliant hybrid zero dynamics to achieve stable, fast running on MABEL. *The International Journal of Robotics Research*, 32(3):324–345, Mar. 2013.
- [28] T. Tamada, W. Ikarashi, D. Yoneyama, K. Tanaka, Y. Yamakawa, T. Senoo, and M. Ishikawa. High-speed bipedal robot running using high-speed visual feedback. In *2014 IEEE-RAS International Conference on Humanoid Robots*, pages 140–145, Nov 2014.
- [29] M. Vukobratovic and B. Borovac. Zero-moment point? thirty five years of its life. *International Journal of Humanoid Robotics*, 1(1):157–173, 2004.
- [30] H. Zhao, A. Hereid, W. I. Ma, and A. D. Ames. Multi-contact bipedal robotic locomotion. *Robotica*, FirstView:1–35, 2 2016.
- [31] H. Zhao, S. Yadukumar, and A. Ames. Bipedal robotic running with partial hybrid zero dynamics and human-inspired optimization. In *IEEE/RSJ International Conference on Intelligent Robots and Systems (IROS)*, pages 1821–1827, Oct 2012.